The Analysis of Downward Terrestrial Gamma-ray Flashes Using a Large-area Cosmic Ray Detector

Jackson Remington
Ph.D. Thesis Defense
Telescope Array Project
Department of Physics and Astronomy, University of Utah

Telescope Array Project

R.U. Abbasi[1], T. Abu-Zayyad[1,2], M. Allen[2], Y. Arai[3], R. Arimura[3], E. Barcikowski[2], J.W. Belz[2], D.R. Bergman[2], S.A. Blake[2], I. Buckland[2], R. Cady[2], B.G. Cheon[4], J. Chiba[5], M. Chikawa[6], T. Fujii[7], K. Fujisue[6], K. Fujita[3], R. Fujiwara[3], M. Fukushima[6], R. Fukushima[3], G. Furlich[2], N. Globus[8,9,10], R. Gonzalez[2], W. Hanlon[2], M. Hayashi[11], N. Hayashida[12], K. Hibino[12], R. Higuchi[6], K. Honda[13], D. Ikeda[12], T. Inadomi[14], N. Inoue[15], T. Ishii[13], H. Ito[8], D. Ivanov[2], H. Iwakura[14], A. Iwasaki[3], H.M. Jeong[16], S. Jeong[16], C.C.H. Jui[2], K. Kadota[17], F. Kakimoto[12], O. Kalashev[18], K. Kasahara[19], S. Kasami[20], H. Kawai[21], S. Kawakami[3], S. Kawana[15], K. Kawata[6], I. Kharuk[18], E. Kido[8], H.B. Kim[4], J.H. Kim[2], J.H. Kim[2], M.H. Kim[16], S.W. Kim[16], Y. Kimura[3], S. Kishigami[3], Y. Kubota[14], S. Kurisu[14], V. Kuzmin[*18], M. Kuznetsov[18,22], Y.J. Kwon[23], K.H. Lee[16], B. Lubsandorzhiev[18], J.P. Lundquist[2,24], K. Machida[13], H. Matsumiya[3], T. Matsuyama[3], J.N. Matthews[2], R. Mayta[3], M. Minamino[3], K. Mukai[13], I. Myers[2], S. Nagataki[8], K. Nakai[3], R. Nakamura[14], T. Nakamura[25], T. Nakamura[14], Y. Nakamura[14], A. Nakazawa[14], E. Nishio[20], T. Nonaka[6], H. Oda[3], S. Ogio[3,26], M. Ohnishi[6], H. Ohoka[6], Y. Oku[20], T. Okuda[27], Y. Omura[3], M. Ono[8], R. Onogi[3], A. Oshima[3], S. Ozawa[28], I.H. Park[16], M. Potts[2], M.S. Pshirkov[18,29], J. Remington[2], D.C. Rodriguez[2], G.I. Rubtsov[18], D. Ryu[30], H. Sagawa[6], R. Sahara[3], Y. Saito[14], N. Sakaki[6], T. Sako[6], N. Sakurai[3], K. Sano[14], K. Sato[3], T. Seki[14], K. Sekino[6], P.D. Shah[2], Y. Shibasaki[14], F. Shibata[13], N. Shibata[20], T. Shibata[6], H. Shimodaira[6], B.K. Shin[30], H.S. Shin[6], D. Shinto[20], J.D. Smith[2], P. Sokolsky[2], N. Sone[14], B.T. Stokes[2], T.A. Stroman[2], Y. Takagi[3], Y. Takahashi[3], M. Takamura[5], M. Takeda[6], R. Takeishi[6], A. Taketa[31], M. Takita[6], Y. Tameda[20], H. Tanaka[3], K. Tanaka[32], M. Tanaka[33], Y. Tanoue[3], S.B. Thomas[2], G.B. Thomson[2], P. Tinyakov[18,22], I. Tkachev[18], H. Tokuno[34], T. Tomida[14], S. Troitsky[18], R. Tsuda[3], Y. Tsunesada[3,26], Y. Uchihori[35], S. Udo[12], T. Uehama[14], F. Urban[36], T. Wong[2], K. Yada[6], M. Yamamoto[14], K. Yamazaki[12], J. Yang[37], K. Yashiro[5], F. Yoshida[20], Y. Yoshioka[14], Y. Zhezher[6,18], and Z. Zundel[2]

[1] *Department of Physics, Loyola University Chicago, Chicago, Illinois, USA*
[2] *High Energy Astrophysics Institute and Department of Physics and Astronomy, University of Utah, Salt Lake City, Utah, USA*
[3] *Graduate School of Science, Osaka City University, Osaka, Osaka, Japan*
[4] *Department of Physics and The Research Institute of Natural Science, Hanyang University, Seongdong-gu, Seoul, Korea*
[5] *Department of Physics, Tokyo University of Science, Noda, Chiba, Japan*
[6] *Institute for Cosmic Ray Research, University of Tokyo, Kashiwa, Chiba, Japan*
[7] *The Hakubi Center for Advanced Research and Graduate School of Science, Kyoto University, Kitashirakawa-Oiwakecho, Sakyo-ku, Kyoto, Japan*
[8] *Astrophysical Big Bang Laboratory, RIKEN, Wako, Saitama, Japan*
[9] *Center for Computational Astrophysics, Flatiron Institute,Simons Foundation, New York, New York, USA*
[10] *ELI Beamlines, Institute of Physics, Czech Academy of Sciences, Dolni Brezany, Czech Republic*
[11] *Information Engineering Graduate School of Science and Technology, Shinshu University, Nagano, Nagano, Japan*
[12] *Faculty of Engineering, Kanagawa University, Yokohama, Kanagawa, Japan*
[13] *Interdisciplinary Graduate School of Medicine and Engineering, University of Yamanashi, Kofu, Yamanashi, Japan*
[14] *Academic Assembly School of Science and Technology Institute of Engineering, Shinshu University, Nagano, Nagano, Japan*
[15] *The Graduate School of Science and Engineering, Saitama University, Saitama, Saitama, Japan*
[16] *Department of Physics, SungKyunKwan University, Jang-an-gu, Suwon, Korea*
[17] *Department of Physics, Tokyo City University, Setagaya-ku, Tokyo, Japan*
[18] *Institute for Nuclear Research of the Russian Academy of Sciences, Moscow, Russia*
[19] *Faculty of Systems Engineering and Science, Shibaura Institute of Technology, Minato-ku, Tokyo, Japan*
[20] *Department of Engineering Science, Faculty of Engineering, Osaka Electro-Communication University, Neyagawa-shi, Osaka, Japan*
[21] *Department of Physics, Chiba University, Chiba, Chiba, Japan*
[22] *Service de Physique Théorique, Université Libre de Bruxelles, Brussels, Belgium*
[23] *Department of Physics, Yonsei University, Seodaemun-gu, Seoul, Korea*
[24] *Center for Astrophysics and Cosmology, University of Nova Gorica, Nova Gorica, Slovenia*
[25] *Faculty of Science, Kochi University, Kochi, Kochi, Japan*
[26] *Nambu Yoichiro Institute of Theoretical and Experimental Physics, Osaka City University, Osaka, Osaka, Japan*
[27] *Department of Physical Sciences, Ritsumeikan University, Kusatsu, Shiga, Japan*
[28] *Quantum ICT Advanced Development Center, National Institute for Information and Communications Technology, Koganei, Tokyo, Japan*
[29] *Sternberg Astronomical Institute, Moscow M.V. Lomonosov State University, Moscow, Russia*
[30] *Department of Physics, School of Natural Sciences, Ulsan National Institute of Science and Technology, UNIST-gil, Ulsan, Korea*
[31] *Earthquake Research Institute, University of Tokyo, Bunkyo-ku, Tokyo, Japan*
[32] *Graduate School of Information Sciences, Hiroshima City University, Hiroshima, Hiroshima, Japan*
[33] *Institute of Particle and Nuclear Studies, KEK, Tsukuba, Ibaraki, Japan*
[34] *Graduate School of Science and Engineering, Tokyo Institute of Technology, Meguro, Tokyo, Japan*
[35] *Department of Research Planning and Promotion, Quantum Medical Science Directorate, National Institutes for Quantum and Radiological Science and Technology, Chiba, Chiba, Japan*
[36] *CEICO, Institute of Physics, Czech Academy of Sciences, Prague, Czech Republic*
[37] *Department of Physics and Institute for the Early Universe, Ewha Womans University, Seodaaemun-gu, Seoul, Korea*

TA / LMA Collaboration

R. Abbasi[1], J. Belz[2], R. LeVon[2], P. Krehbiel[3],
J. Remington[2], W. Rison[3], D. Rodeheffer[3],
M. Stanley[3], K. Smout[2]

[1] Department of Physics, Loyola University
[2] Department of Physics, University of Utah
[3] Langmuir Laboratory, New Mexico Institute of Mining and Technology

The work reported here was partially supported by National Science Foundation grants AGS-1205727, AGS-1613260, AGS-1720600, and AGS-1844306. We greatly acknowledge the contributions of our colleagues at the Telescope Array Cosmic Ray Observatory. We also thank VAISALA for providing NLDN data under their academic research use policy.

Outline

1. **Background of Terrestrial Gamma-ray Flashes (TGFs)**
   a. History of TGFs
   b. Thundercloud and lightning anatomy
   c. TGF production and development
2. Instrumentation
   a. Telescope Array Surface Detectors
   b. Lightning detectors
3. TGF Observations at Telescope Array
   a. Previous observations 2008-2016
   b. 2018 TGFs: observations
   c. 2018 TGFs: analysis
   d. 2018 TGFs: interpretation
4. Conclusion

TGF History: A Series of Happy Accidents

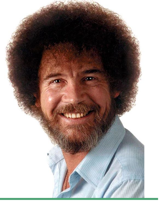

1963 Vela satellites launched to search for gamma-ray signatures of nuclear weapons testing

1973 Vela satellites report extra-galactic gamma-ray bursts (GRBs)

1994 BATSE detector on the Compton Gamma Ray Observatory detects radiation from Earth during thunderstorms, later called TGFs

2013 'Bursts' of events are seen by Telescope Array during lightning flashes, later recognized as TGFs

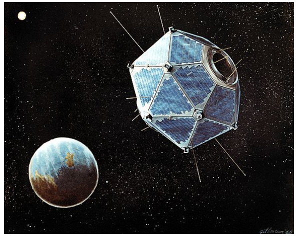

NASA

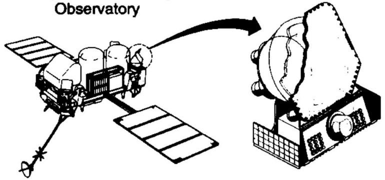

Fishman, et al. (1994), Science (264), 1313

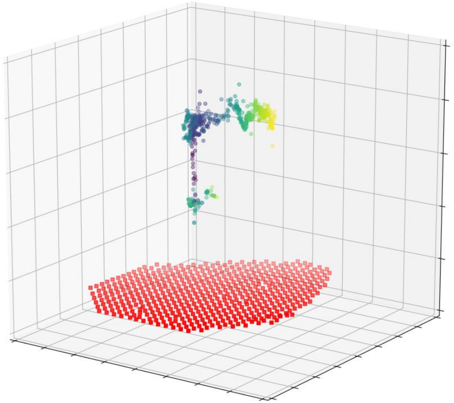

Terrestrial Gamma-ray Flashes (TGFs)

TGFs are electromagnetic showers produced during lightning flashes

Satellite observations of TGFs:

- Contain 10^{15}-10^{19} photons
- Have characteristic gamma-ray energy of 7 MeV
- Occur in the initial stages of lightning
- Durations of 10s-100s of μs

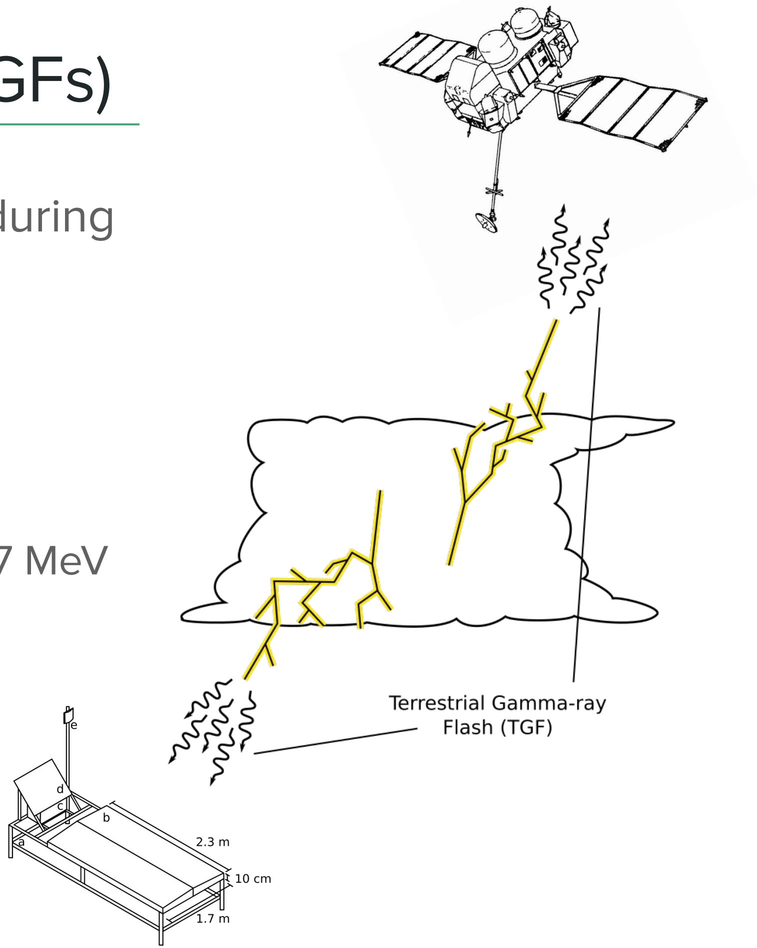

Thundercloud Anatomy

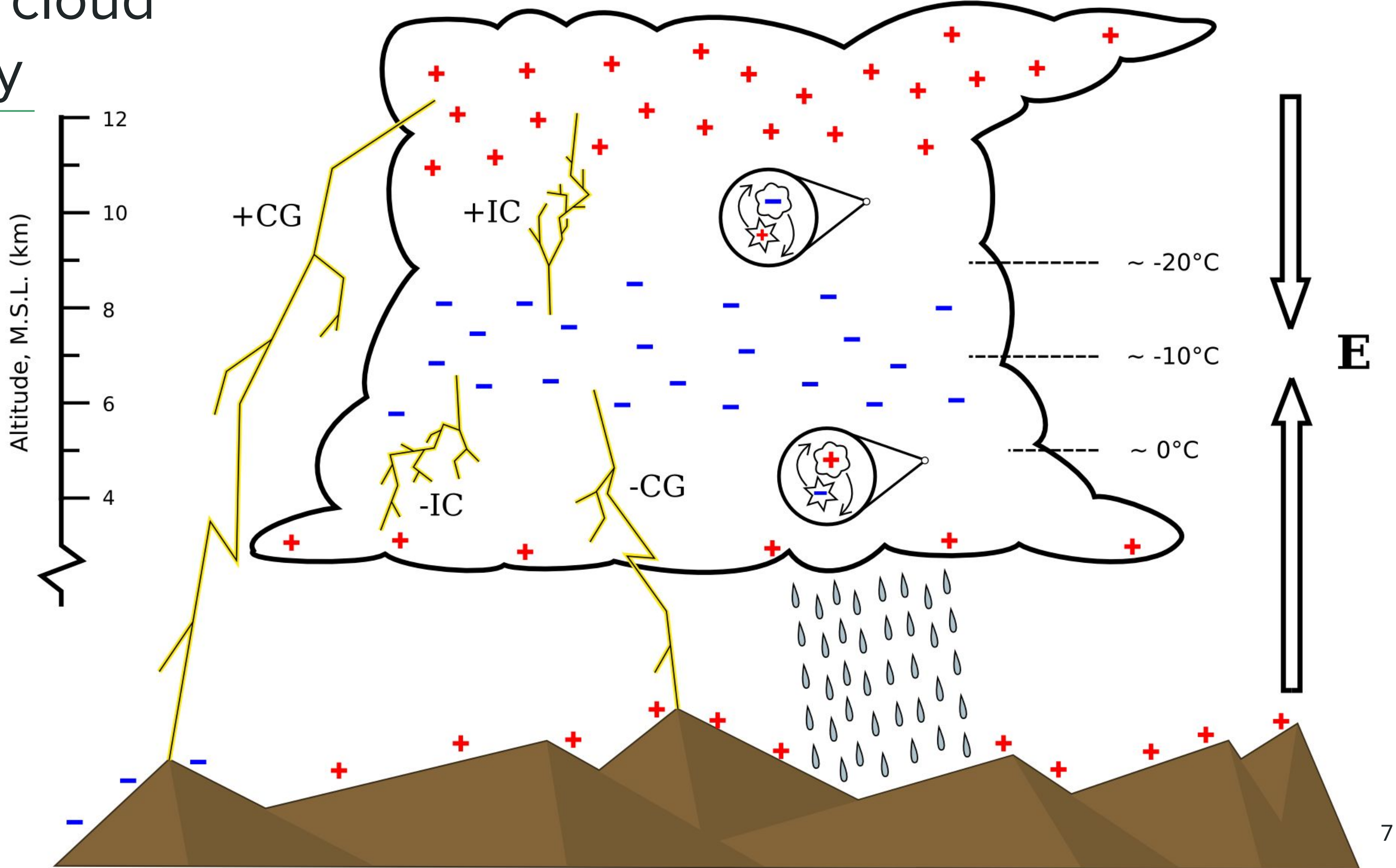

Stages of Lightning

1. Leader stage creates a conducting pathway
   - Average leader speed 10^5-10^6 m/s
   - 8 ms leader time
2. Once a pathway is formed, the storm “shorts out”
3. Bright return stroke(s) discharge the electric field
   - Can occur multiple times in a single flash (15 ms separation)

40,000 FPS camera:

➔ 1 ms of lightning = 1.3 s of video

Stages of Lightning

- Leaders are hot, conducting channels of air allowing current to flow
  - Leaders advance discretely in ~50 m steps at 10^5-10^6 m/s
  - TGF production is associated with the leader stage
- Streamers are non-conducting systems of ionized air
- The bright return stroke(s) occur once the leader "shorts out" charge regions

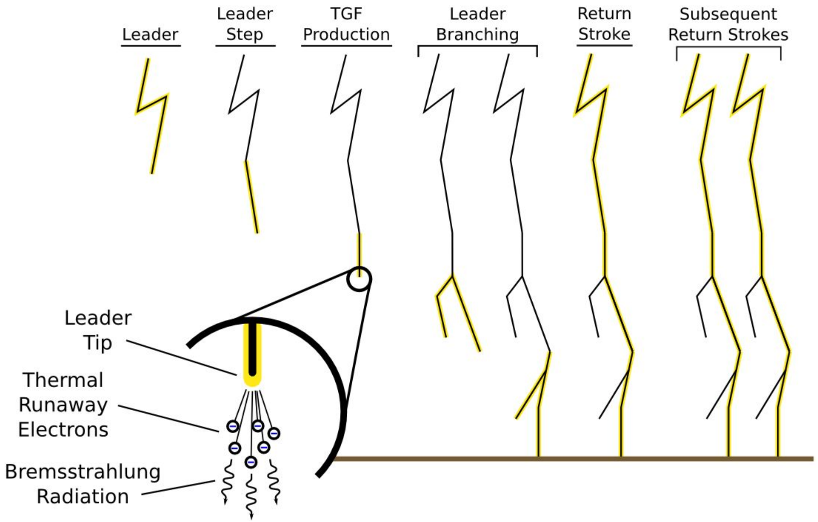

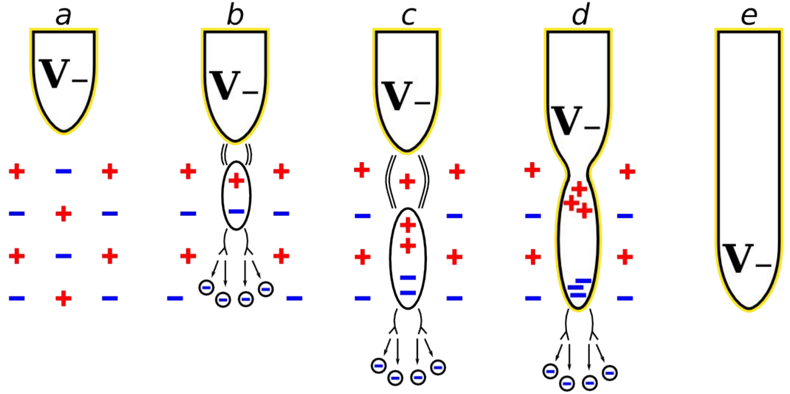

Leader stepping process (left)

- (a): Electrons concentrate in the leader tip and generate strong fields
- (b): Charges separate ahead of the leader and generate streamer systems
- (c): The air heats up and becomes fully conducting as a disconnected 'space stem'
- (d): The stem reconnects with the existing leader
- (e): Potential transfers to the new leader step and the process repeats

TGF Production and Development

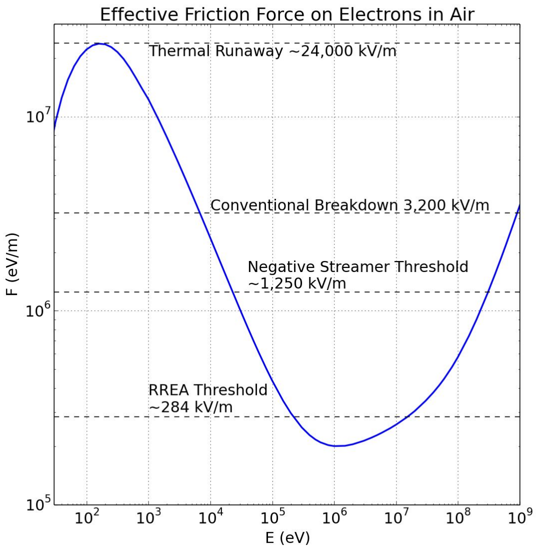

- Electrons gain energy from the thunderstorm's ambient electric field
- Lose energy due to atmospheric interactions - primarily bremsstrahlung radiation and ionization
- Electrons above the curve gain more energy from the applied electric field than they lose due to atmospheric interactions

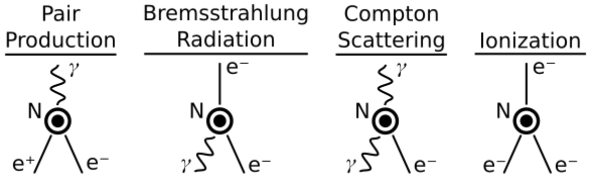

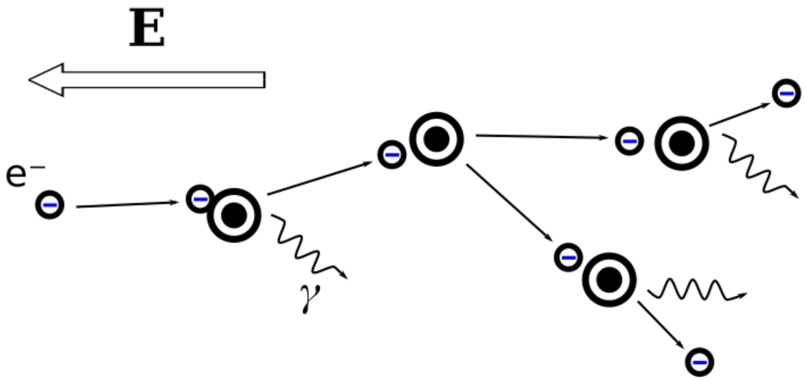

TGF Production and Development

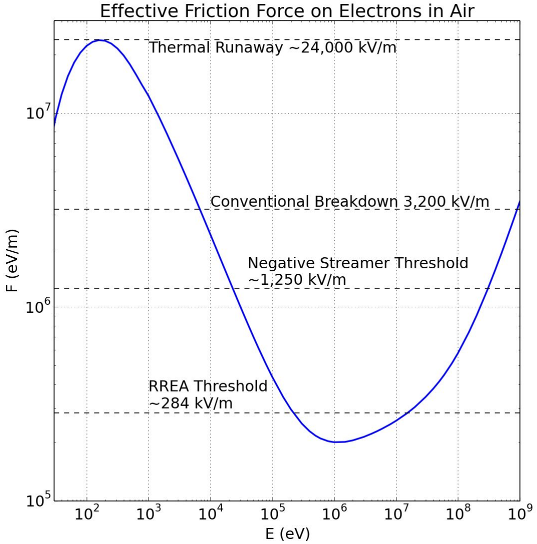

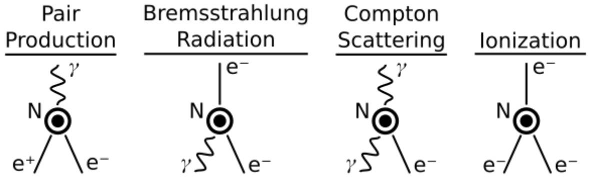

- Electrons above the curve gain more energy from the applied electric field than they lose due to atmospheric interactions
- Cascades of particles above the curve multiply quickly, called relativistic runaway electron avalanches (RREA)
- Electrons must exist above the curve in abundance in order to seed RREA cascades
    - Cosmic ray secondaries
    - Cold runaway mechanisms (supported by this study)

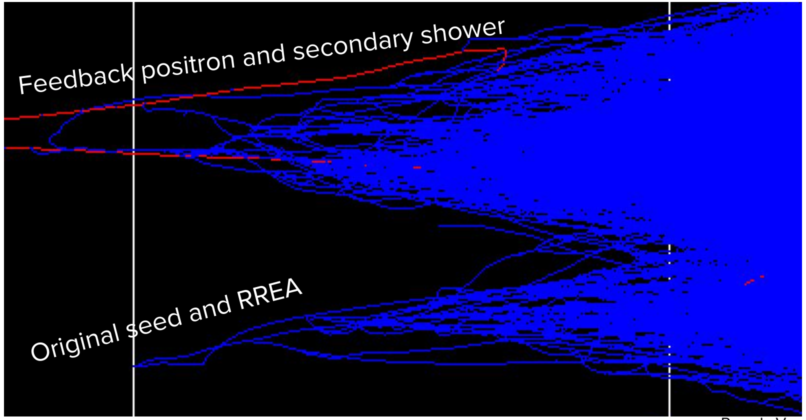

Ryan LeVon

Backscattered positrons and photons can seeed additional showers in a process called feedback, greatly amplifying the shower fluence and duration

TGF Production and Development

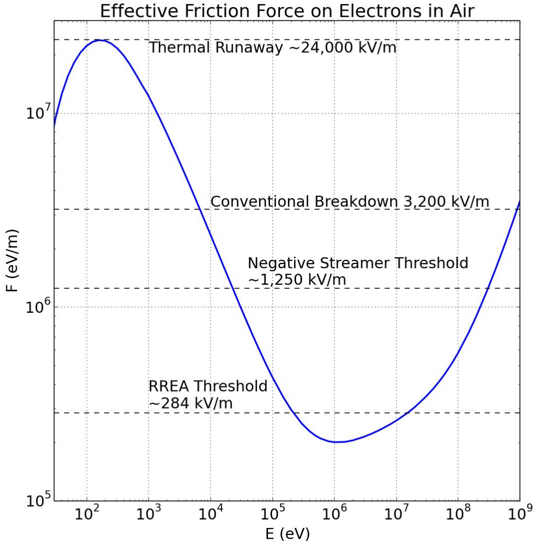

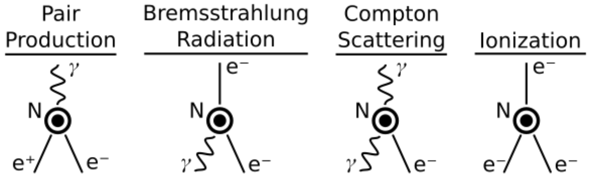

- Our observations suggest that RREA is seeded during leader steps
  - RREA develops in the larger-scale thunderstorm fields (~10^5 V/m)
  - E field enhanced near leader tips (~10^6 V/m)
  - E field enhanced further by advancing streamer systems (~10^7 V/m)
- Cold electrons are ejected at relativistic speeds (~10^6 eV)

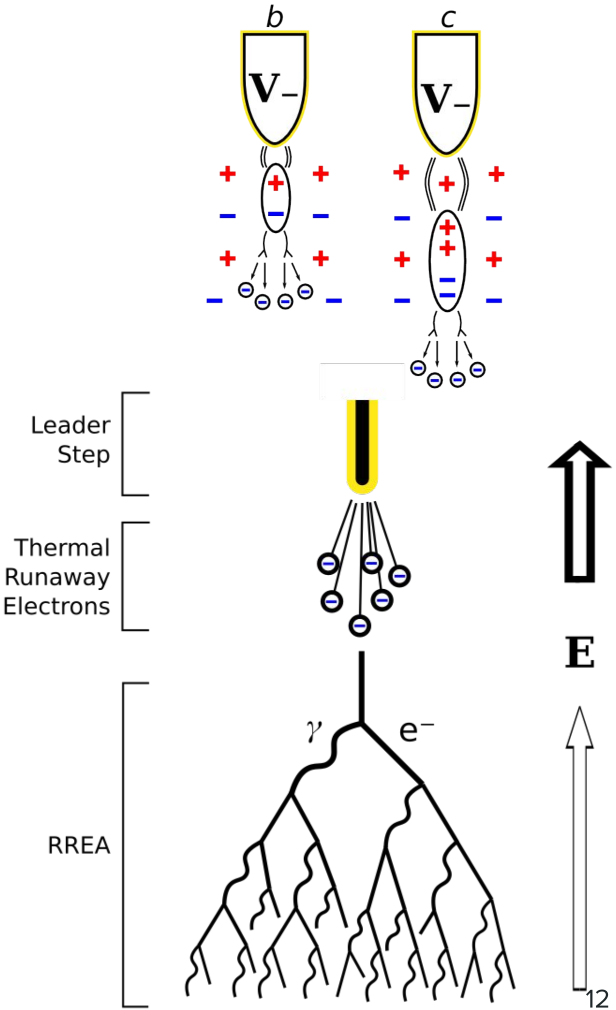

Outline

1. Background of Terrestrial Gamma-ray Flashes (TGFs)
    a. History of TGFs
    b. Thundercloud and lightning anatomy
    c. TGF production and development
2. **Instrumentation**
    a. Telescope Array Surface Detectors
    b. Lightning detectors
3. TGF Observations at Telescope Array
    a. Previous observations 2008-2016
    b. 2018 TGFs: observations
    c. 2018 TGFs: analysis
    d. 2018 TGFs: interpretation
4. Conclusion

Instrumentation: Telescope Array

- 507 scintillation detectors (SDs) covering the 700 km^2 main array
  - Able to capture the entire ground-level footprint
- TASDs contain two layers of plastic scintillator for detecting charged particles
  - Efficient for charged particle detection
  - Inefficient for neutral gamma-rays
- Energy deposit in the form of fluorescence light is captured for each layer and counted on local electronics.

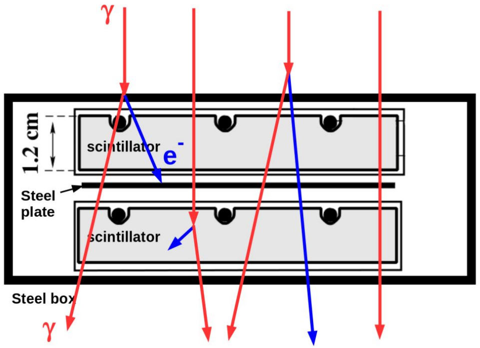

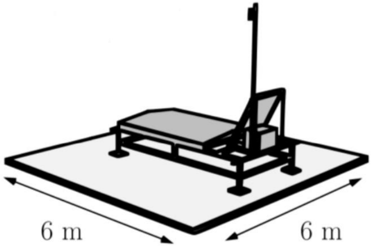

Dmitri Ivanov

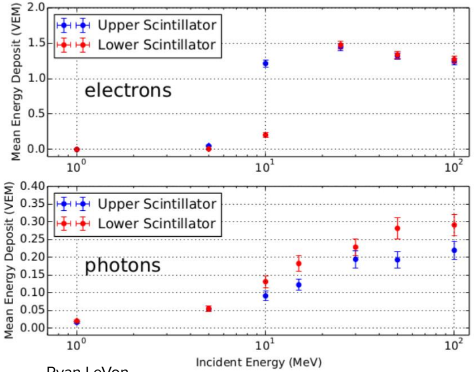

Ryan LeVon

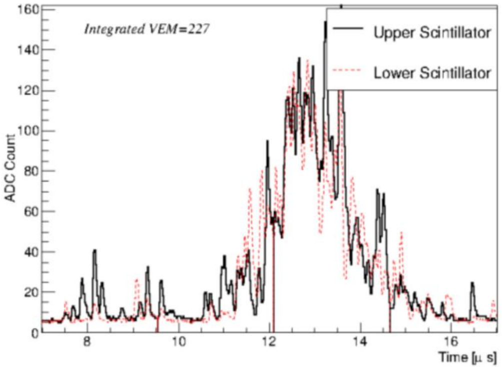

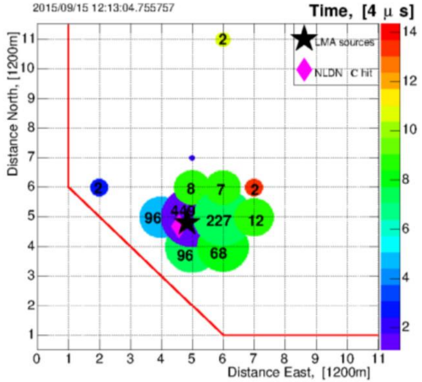

Instrumentation: gamma-ray detection

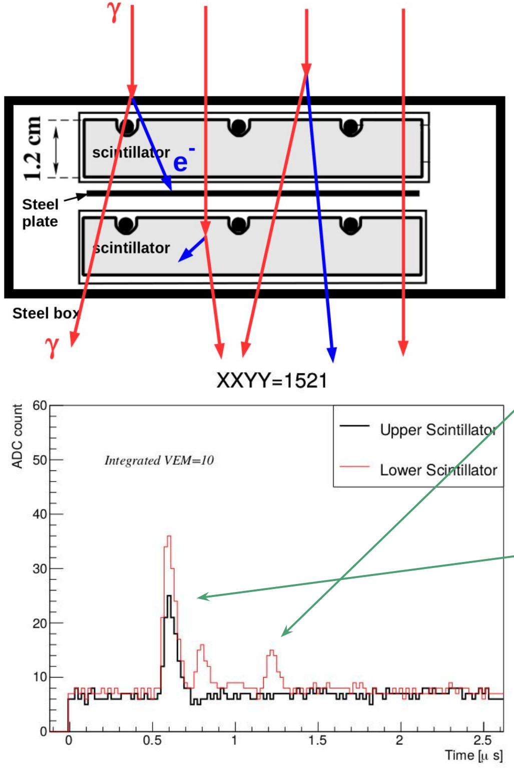

- In some cases, TASD waveforms show individual particle hits
  - Energy deposit is consistent with 1 vertical equivalent muon (VEM), or ~2 MeV/cm
- Minimum energy case:
  - A Compton-scattered electron deposits all of its energy into one layer of scintillator (2.4 MeV for 1.2 cm)
  - If produced inside the scintillator itself (no energy loss to exclosure), the minimum-energy photon had 2.4+0.2=**2.6 MeV**
- Penetrating case:
  - An electron penetrates both scintillators and the steel separating plate (~1.4 MeV loss)
  - Minimum photon energy = 2.4+1.4+2.4+0.2=**6.4 MeV**

(Keep in mind these are lower limits - the likelihood of grazing angles means the original photons probably had more energy)

Instrumentation: Lightning Detectors

- Lightning Mapping Array (LMA) locates lightning activity sources in 3D
  - VHF 60-66 MHz
- Sferic sensors measure changes in the local electric field
  - Slow antennas (SAs) measure overall field development (τ = 10 s)
  - Fast antennas (FAs) measure quick fluctuations (τ = 100 μs)
- Broadband interferometer locates lightning activity sources in 2D, higher resolution
  - 20-80 MHz

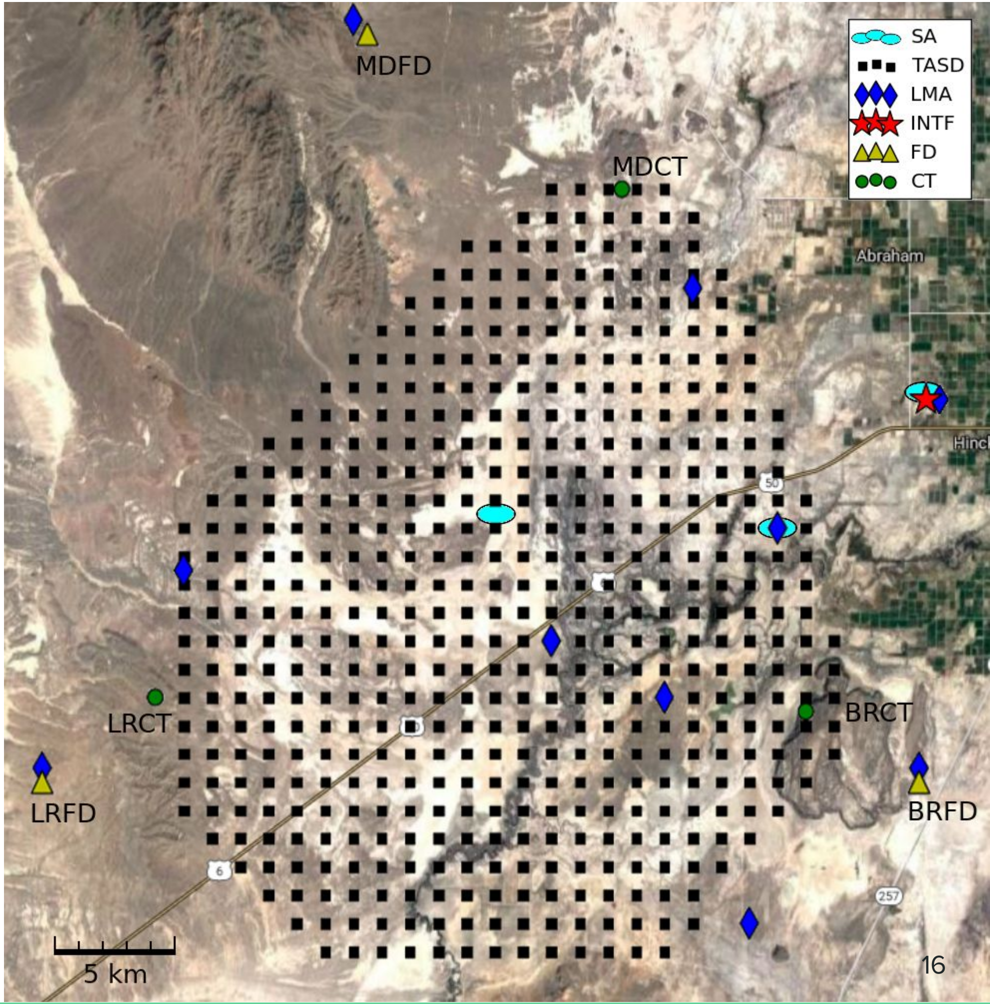

Outline

1. Background of Terrestrial Gamma-ray Flashes (TGFs)
    a. History of TGFs
    b. Thundercloud and lightning anatomy
    c. TGF production and development
2. Instrumentation
    a. Telescope Array Surface Detectors
    b. Lightning detectors
3. **TGF Observations at Telescope Array**
    a. Previous observations 2008-2016
    b. 2018 TGFs: observations
    c. 2018 TGFs: analysis
    d. 2018 TGFs: interpretation
4. Conclusion

Previous TGF Observations at Telescope Array

2008 - 2013

- 10 ‘burst’ events defined as triggering TASDs 3+ times within 1 ms
  - Long, complex signals
- Many occur during lightning flashes recorded by National Lightning Detection Network (NLDN)
  - Nationwide commercial lightning data with ~300 m resolution
  - Some trajectories point back to NLDN flash locations

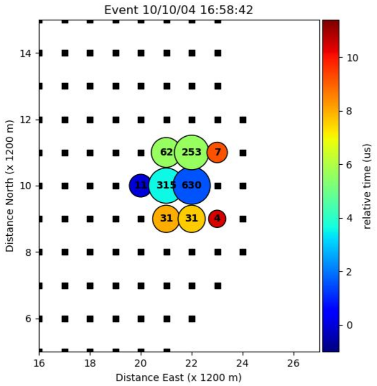

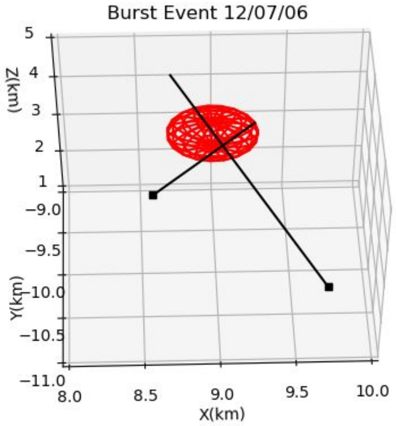

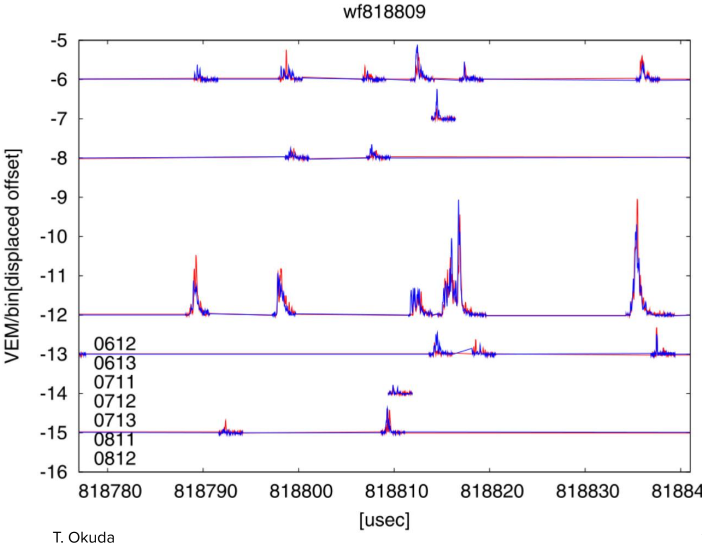

T. Okuda

Previous TGF Observations at Telescope Array

2014 - 2016

- 10 new events after installation of the LMA and slow sferic sensors
- Data shows that TGFs are associated with the very early stages of leader development
- TGFs arrive in bursts lasting hundreds of microseconds

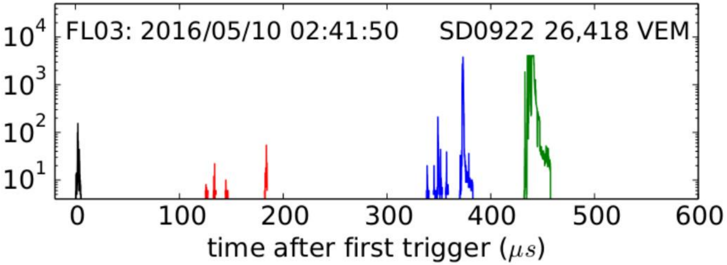

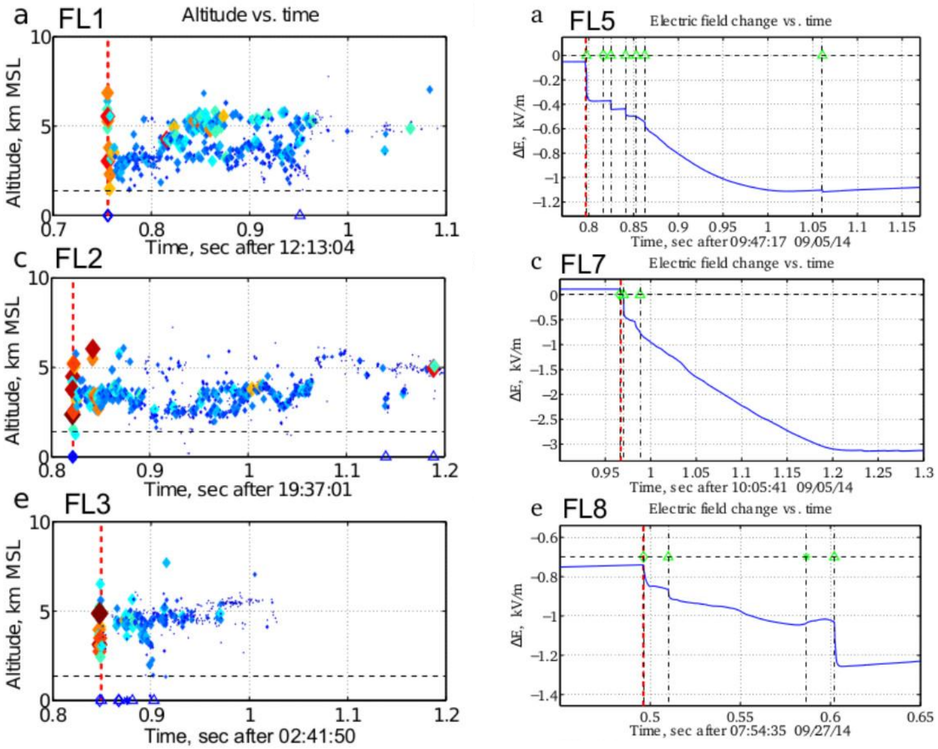

2018 TGFs: Observations

- Four TGFs from August-October 2018
    - TGFs A,C,D consisted of 2 triggers, B was a single trigger.
- All four occurred in the first 1-2 ms of downward negative lightning
    - TGFs A,B,C ended in cloud-to-ground strokes, D was an intracloud flash

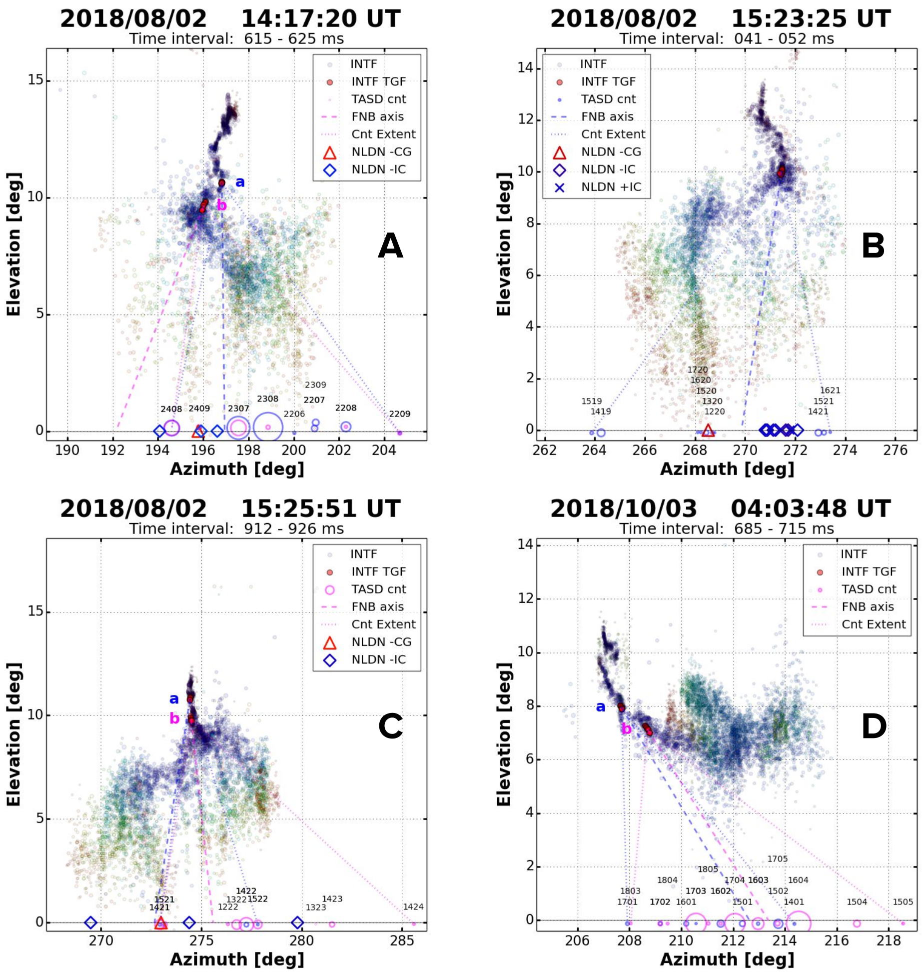

2018 TGFs: Analysis

- INTF does not detect the TGF
- TASDs do not detect lightning
  - Propagation delays result in relative timing differences up to 100 μs (a➔b vs. a➔c)
  - Goal resolution is 1 μs
- TGF altitude depends on source time, which depends on altitude, etc.

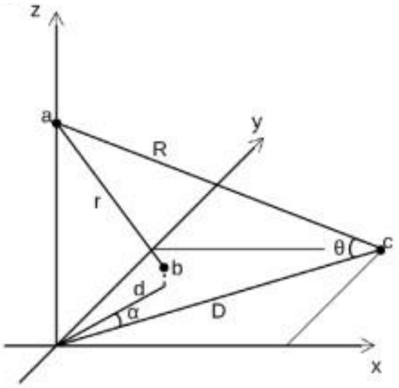

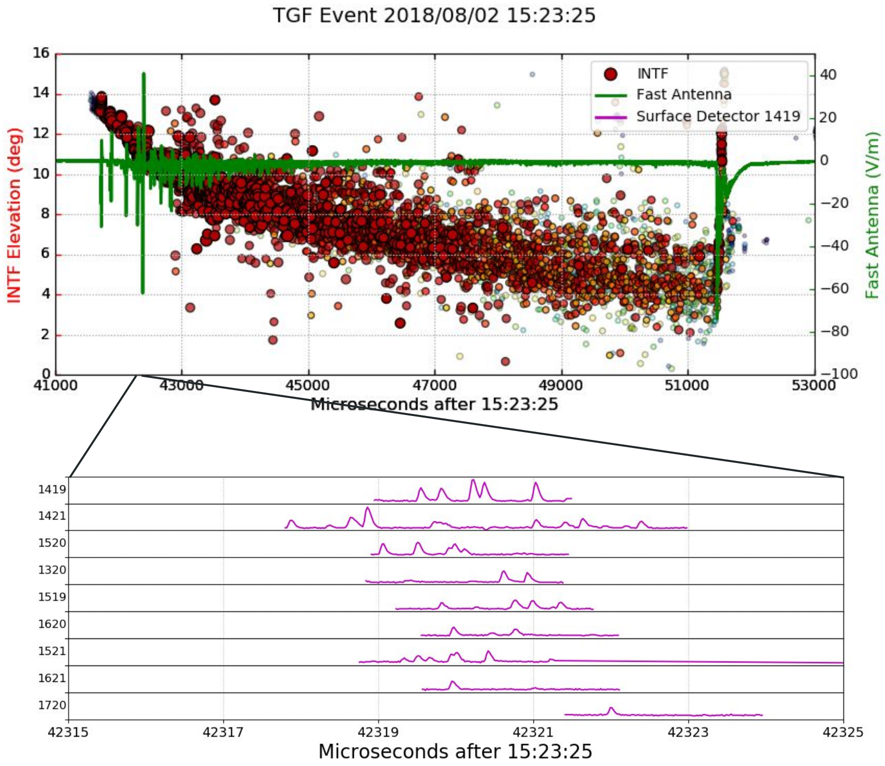

2018 TGFs: Analysis

- Resulting average errors:
  - Horizontal (x,y): 140 m
  - Vertical (z): 25 m
  - Timing (t): 0.6 μs

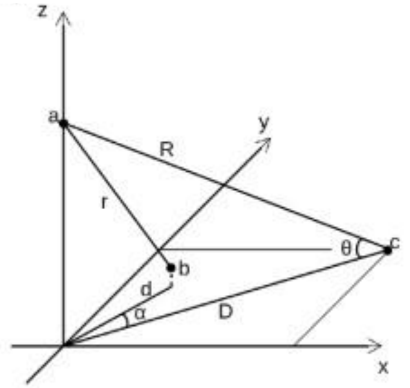

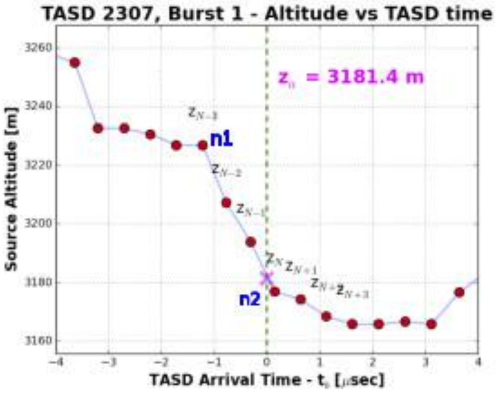

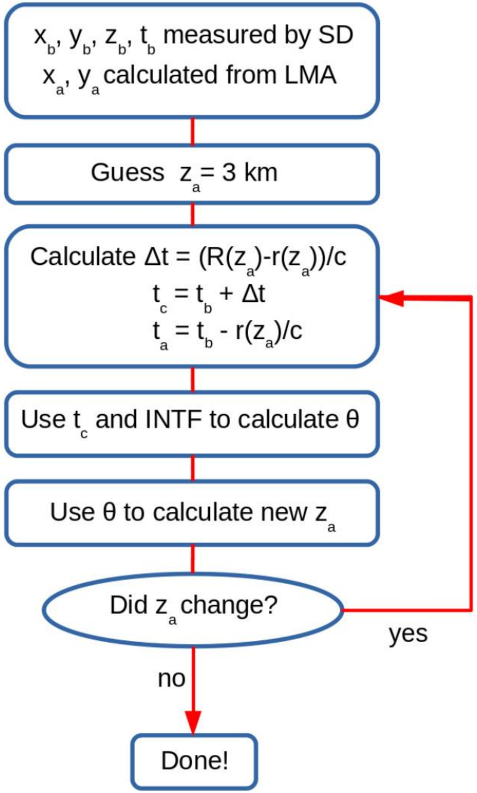

2018 TGFs: Results

Propagation delays removed - TASD, INTF, and sferic data can be directly compared

First ground observations of IBPs and TGFs

The IBPs and TGFs occur during strong leader steps

Timing resolution < 1 μs can identify IBP substructure and breakdown processes

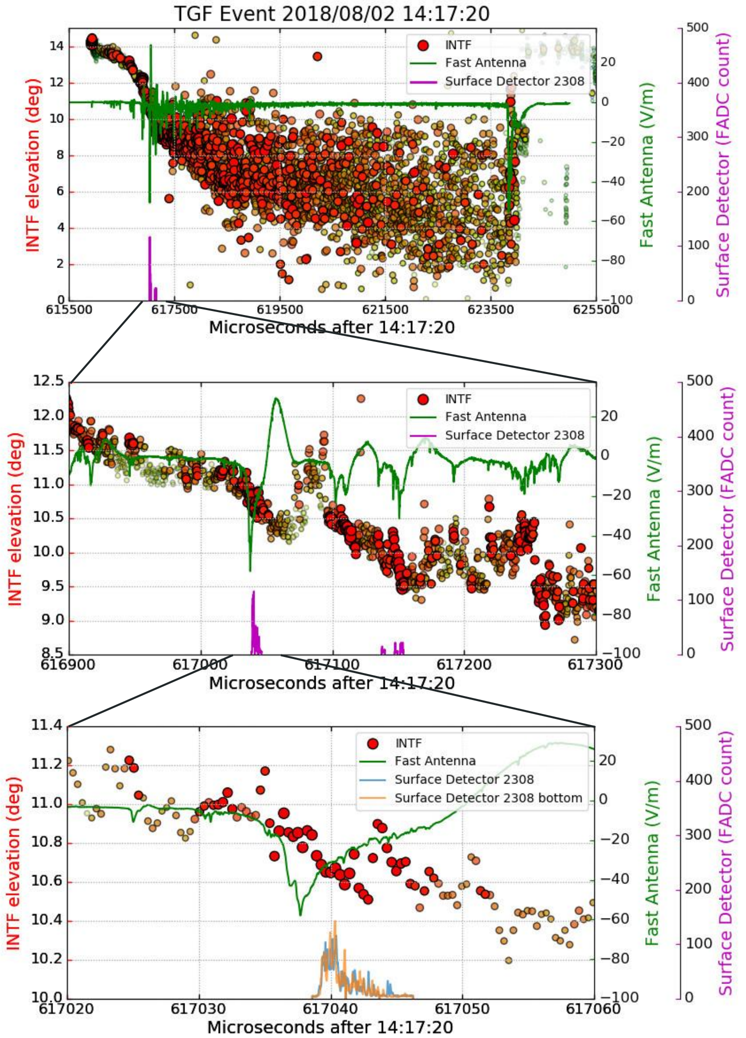

2018 TGFs: Results

- Strongest burst of each TGF occurs during the strongest IBP
- Leader step development is faster, stronger, and more linear
  - Power and speed of leader propagation indicates fast negative breakdown (FNB)
- IBPs also have strong sub-pulses, sometimes correlated with TGF production
- Step discontinuity in leader propagation during each TGF onset

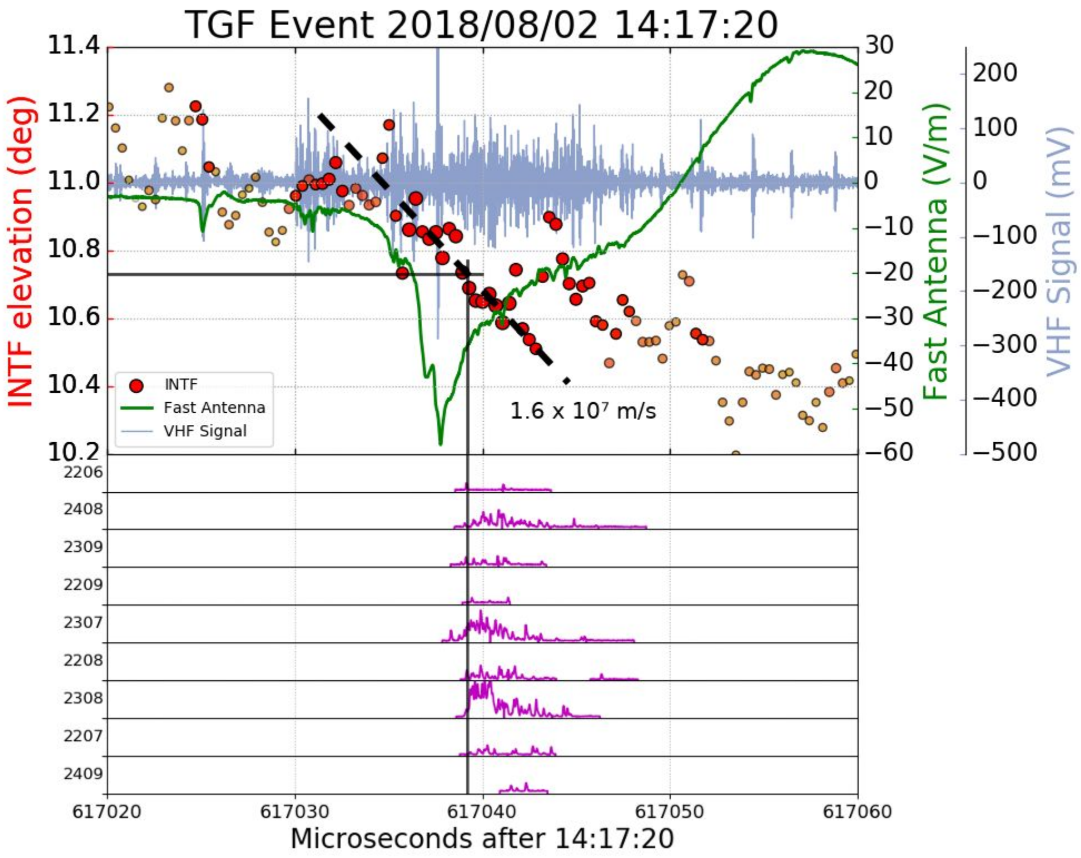

2018 TGFs: Interpretation

- Downward TGFs are produced during strong IBPs and periods of FNB in the early leader steps of downward negative lightning
- **TGF sources have durations of ~3-8 μs**, continuing until FNB dies out
  - Simulations show that the signal durations at the ground reflect the true durations of the source
  - 95% of particles from an instantaneous source arrive in 60 ns
- Since FNB is a streamer-based process, **these results support the cold runaway model** of TGF production
  - Advancing streamer systems enhance local electric fields to the point of seeding RREA

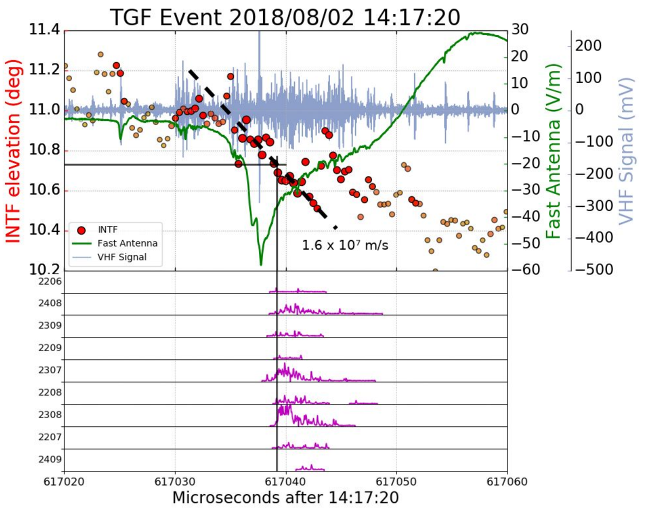

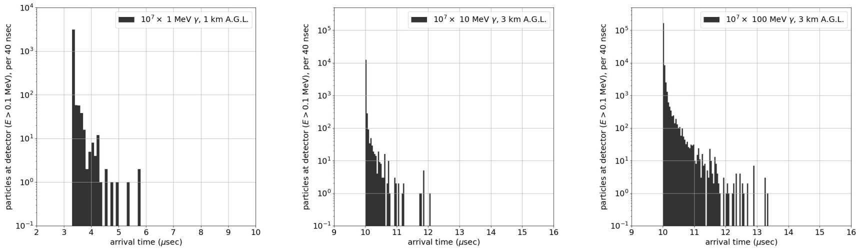

Photon arrival times from an instantaneous source
(data by Ryan LeVon)

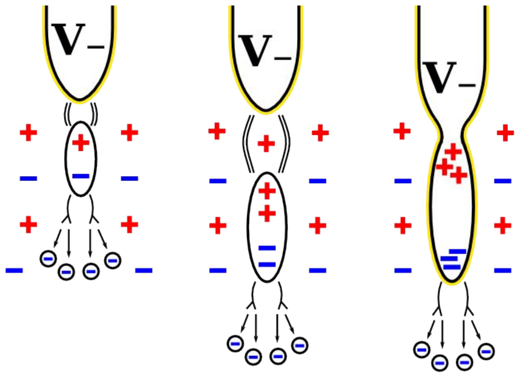

TGF seeding by cold runaway during leader stepping

Outline

1. Background of Terrestrial Gamma-ray Flashes (TGFs)
   a. History of TGFs
   b. Thundercloud and lightning anatomy
   c. TGF production and development
2. Instrumentation
   a. Telescope Array Surface Detectors
   b. Lightning detectors
3. TGF Observations at Telescope Array
   a. Previous observations 2008-2016
   b. 2018 TGFs: observations
   c. 2018 TGFs: analysis
   d. 2018 TGFs: interpretation
4. **Conclusion**

Conclusion

The observations at Telescope Array constitute a significant portion of all downward TGFs

These downward TGFs...

- are **produced in the first 1-2 ms** of downward negative lightning at altitudes of 2.8-3.2 km
- are produced during strong IBPs and streamer-based FNB, **supporting the cold runaway model** of TGF production
- individually **last <10 μs**, but can occur in sequences spanning up to 500 μs
- produce showers at ground level having diameters 3-5 km, corresponding to half-opening angles of 25-40°
- are consistent with simulated showers consisting of 10^{12}-10^{14} photons, with **evidence of some gamma-rays having at least 6.4 MeV**

Future investigations:

- Increase resolution with a second interferometer for stereo measurements
  - Installed 2020
- Additional lightning detector upgrades
  - Electric field mill installed 2021
  - High-speed optical camera installed 2021
- Investigate differences between upward and downward TGFs
  - Downward TGFs have shorter duration, smaller fluence
- Multi-messenger TGFs?

2021/09/11 Flash

- ~6 km footprint diameter
- > 16 GeV in one TASD
- Leader speed ~2.6×10^6 m/s (2 ms)

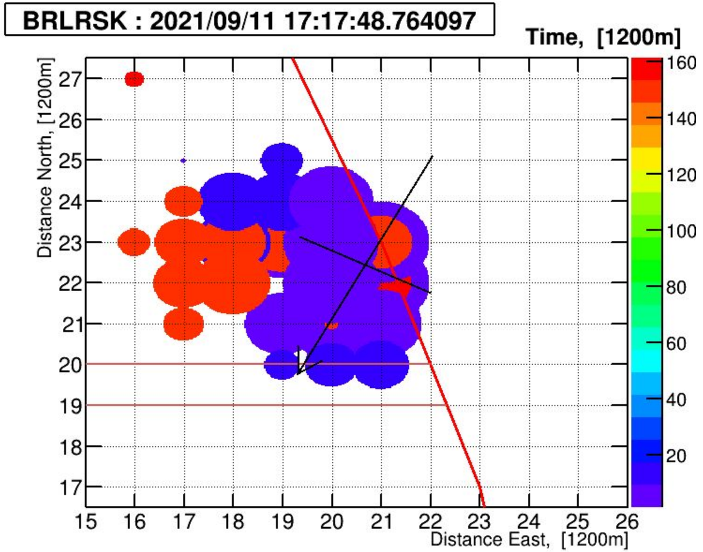

TGF Publications

- Observation of the Origin of Downward Terrestrial Gamma-ray Flashes
  - J. Belz, et al. (2020). *JGR: Atmos, 125* https://doi.org/10.1029/2019JD031940
- Gamma-ray Showers Observed at Ground Level in Coincidence With Downward Lightning Leaders
  - R Abbasi, et al. (2018). *JGR: Atmos, 123* https://doi.org/10.1029/2017JD027931
- The Bursts of High Energy Events Observed by the Telescope Array Surface Detector
  - R. Abbasi, et al. (2017). *Phys. Lett. A, 381* https://dx.doi.org/10.1016/j.physleta.2017.06.022

Telescope Array Publications

- Search for Large-scale Anisotropy on Arrival Directions of Ultra-high-energy Cosmic Rays Observed with the Telescope Array Experiment
  - R. Abbasi, et al. (2020). Astrophys. *J. Lett., 898* https://doi.org/10.3847/2041-8213/aba0bc
- Evidence for a Supergalactic Structure of Magnetic Deflection Multiplets of Ultra-High Energy Cosmic Rays
  - R. Abbasi, et al. (2020). *Astrophys. J., 899* https://doi.org/10.3847/1538-4357/aba26c
- Search for Point Sources of Ultra-High-Energy Photons with the Telescope Array Surface Detector
  - R. Abbasi, et al. (2020). *Monthly Notices of the Royal Astronomical Society, 492* https://doi.org/10.1093/mnras/stz3618
- Search for Ultra-High-Energy Neutrinos with the Telescope Array Surface Detector
  - R. Abbasi, et al. (2020). *J. Exp. Their. Phys., 131* https://doi.org/10.31857/S0044451020080052
- Constraints on the Diffuse Photon Flux with Energies Above 10^{18} eV Using the Surface Detector of the Telescope Array Experiment
  - R. Abbasi, et al. (2019). *J. Astropart. Phys., 110* https://doi.org/10.1016/j.astropartphys.2019.03.003
- Testing a Reported Correlation Between Arrival Directions of Ultra-High-Energy Cosmic Rays and a Flux Pattern From Nearby Starburst Galaxies Using Telescope Array Data
  - R Abbasi, et al. (2019). *Astrophys. J. Lett., 867* https://doi.org/10.3847/2041-8213/aaebf9
- Mass Composition of Ultrahigh-Energy Cosmic Rays with the Telescope Array Surface Detector Data
  - R Abbasi, et al. (2019). *Phys. Rev. D, 99* https://doi.org/10.1103/PhysRevD.99.022002
- Study of Muons from Ultrahigh Energy Cosmic Ray Air Showers Measured With the Telescope Array Experiment
  - R. Abbasi, et al. (2018). *Phys. Rev. D, 98* https://doi.org/10.1103/PhysRevD.98.022002

Supplementary Slides

Supplementary Slides

1. Lightning Leaders
    a. Leader development details
    b. FNB, streamers, and E-field enhancement
    c. EM shower composition
2. Instrumentation details
    a. Telescope Array Surface Detector (TASD)
    b. Lightning Mapping Array (LMA)
    c. Sferic sensors (SA + FA)
    d. Broadband interferometer (INTF)
3. 2018 TGFs
    a. Error analysis details
    b. Results details
    c. Comparison of upward and downward flashes
4. Optical camera footage

Stages of Lightning

- Leaders are hot, conducting channels of ionized air allowing current to flow
  - Leader initiate at the sharp corners of ice crystals
  - Leaders develop discretely in ~50 m steps
  - TGF production is associated with the leader stage
- The bright return stroke(s) occur once the leader creates a pathway between charge regions

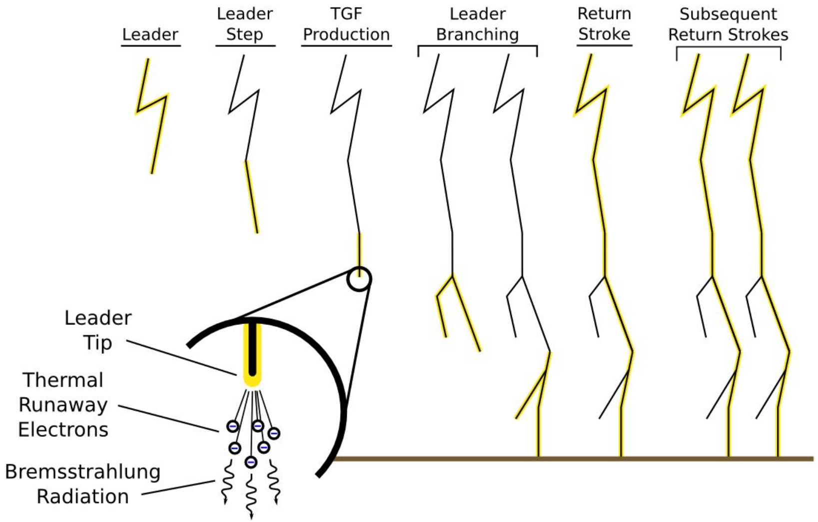

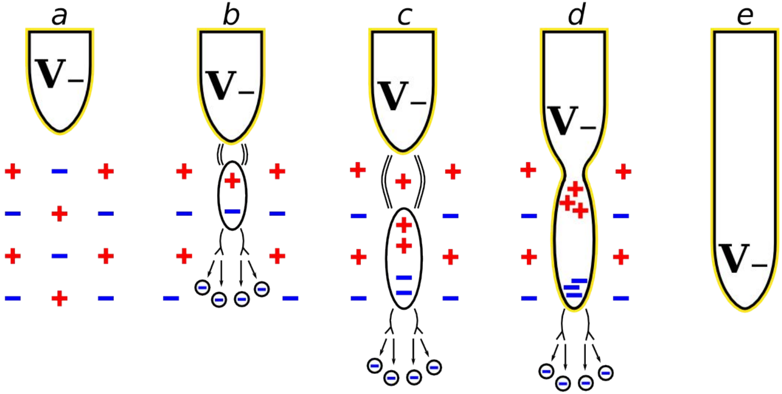

Leader stepping process (left)

- (a): Electrons concentrate in the leader tip and generate strong fields
- (b): Charges separate ahead of the leader and generate streamer systems
- (c): The air heats up and becomes fully conducting as a disconnected ‘space stem’
- (d): The stem reconnects with the existing leader
- (e): Potential transfers to the new leader step and the process repeats

Fast Negative Breakdown (FNB)

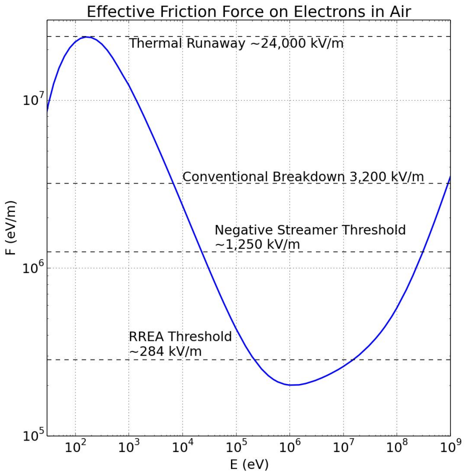

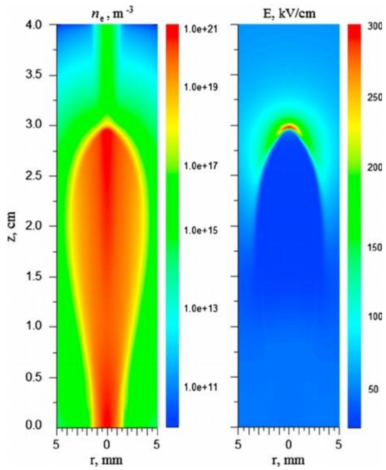

Babich, et al. (2015) *JGR: Atmospheres 120*

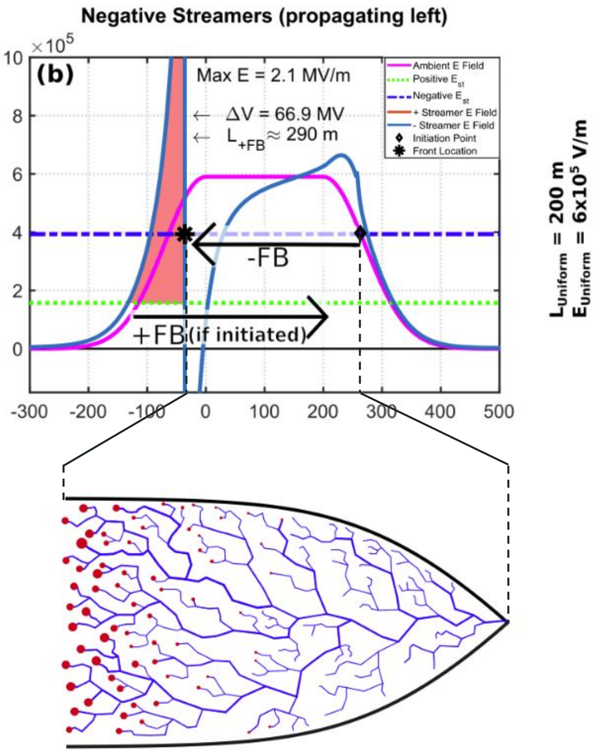

Attanasio, A., da Silva, C., Krehbiel, P. (2021). *unpublished*

Large-scale thunderstorm E field (RREA Threshold):

~2.8 x 10^5 V/m

Leader tip E field enhancement

10^6-10^7 V/m

FNB E field enhancement x10

~10^7 V/m
(cold runaway)

Electromagnetic Showers

Driven EM shower (RREA): ~50% photons ~50% electrons + positrons

Typical EM shower: ~90% photons, ~10% electrons + positrons

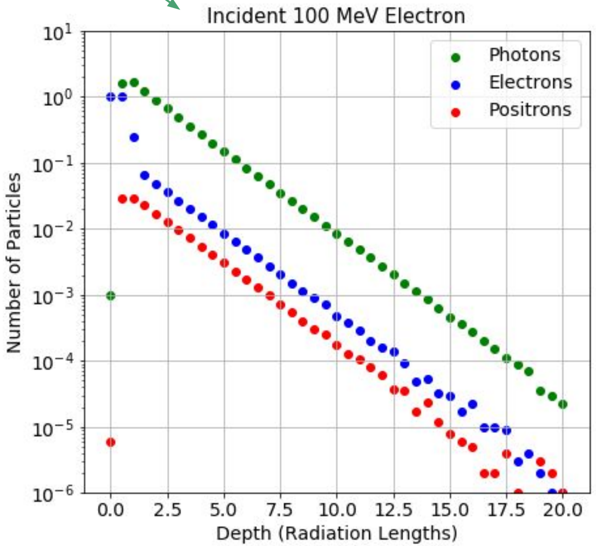

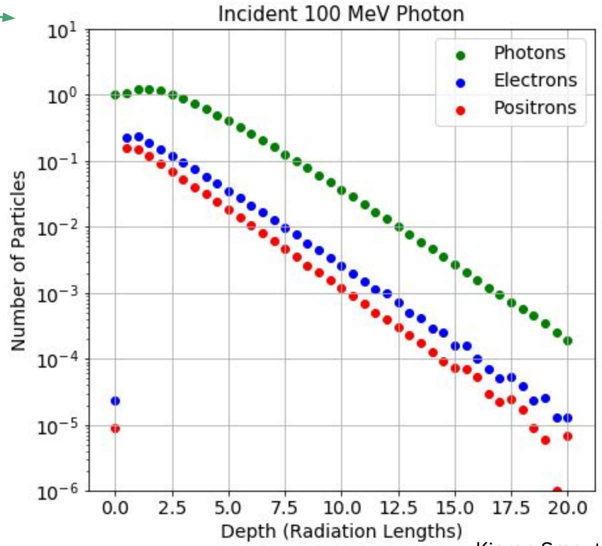

Instrumentation: Telescope Array

- 507 scintillation detectors (SDs) covering the 700 km^2 main array
    - An expansion to 4x size is underway, but data of this study was recorded only on the main array
    - Fluorescence detectors (FDs) data not used in this study
- TASDs contain two layers of plastic scintillator for detecting charged particles.
- Energy deposit in the form of fluorescence light is captured for each layer and counted on local electronics.

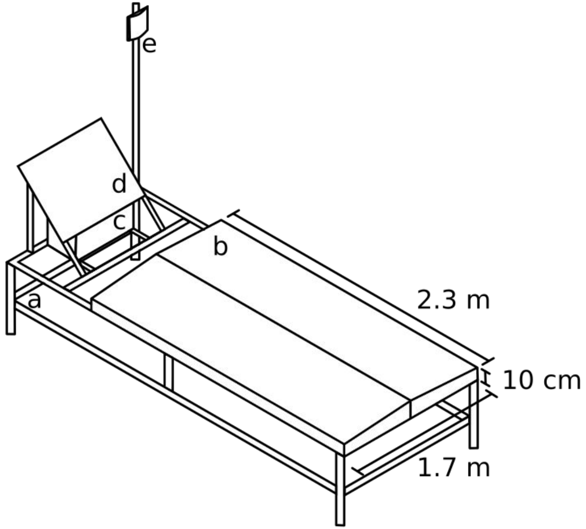

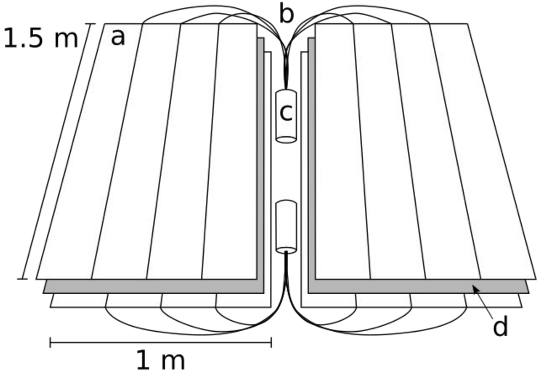

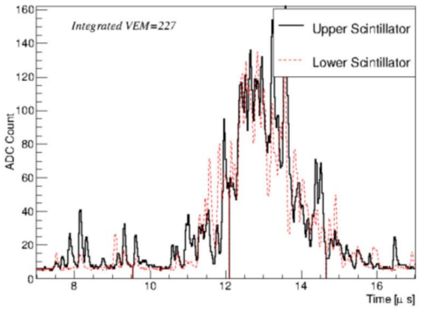

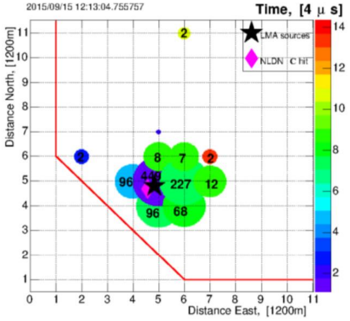

Instrumentation: TASD RF Interference

FL03: 2016/05/10 02:41:50

Cloud-to-ground lightning stroke only 78 m from TASD 0922 caused pedestal and FADC fluctuations (@ ~13 and 15 μs)

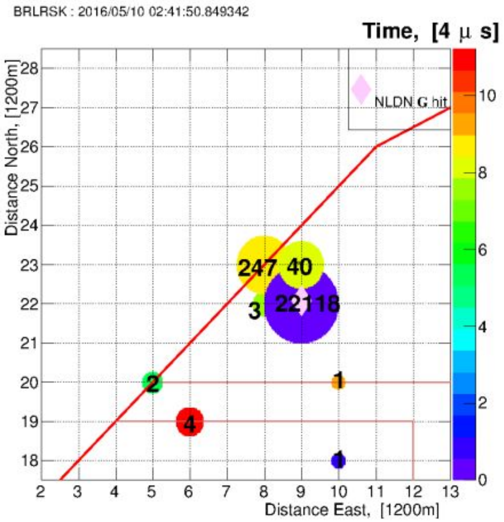

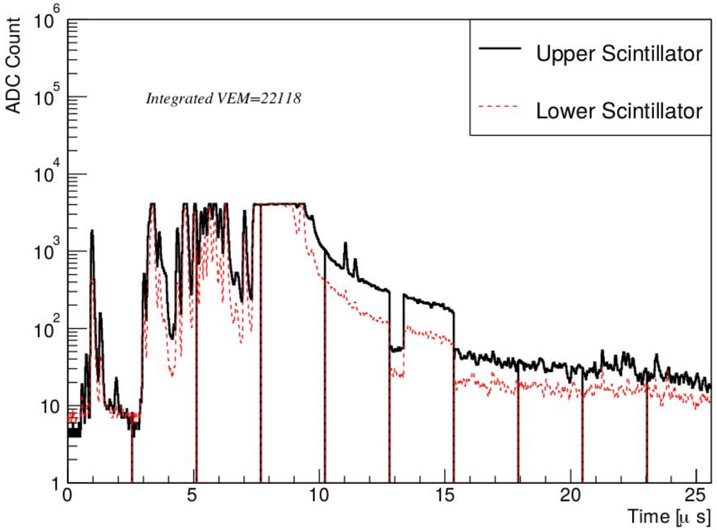

Instrumentation: Lightning Mapping Array (LMA)

- 11 detectors spread over main TA detecting narrow bipolar events
    - Installed 2013 by Langmuir Laboratory for Atmospheric Research
- Time-of-arrival analysis determines 3D locations of individual sources (a few per ms)
- Errors of a similar (larger) array:
    - 40-50 ns in t
    - 10-50 m in x, y
    - 20-100 m in z

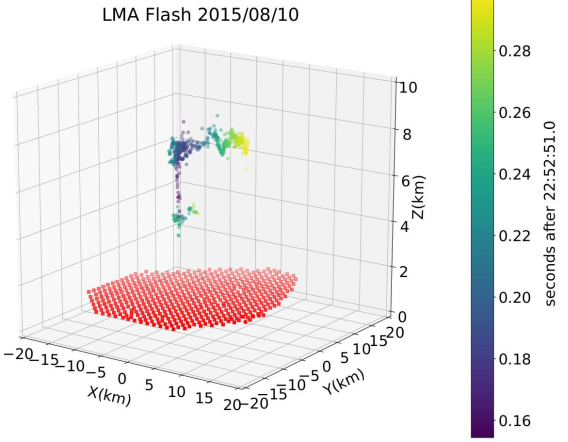

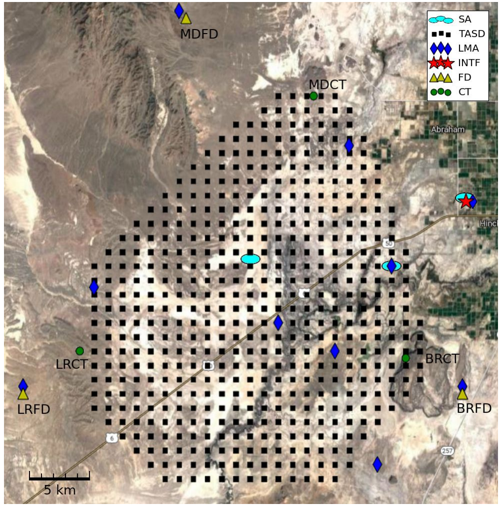

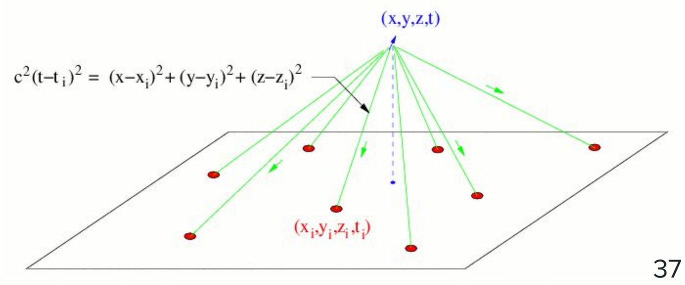

Instrumentation: Sferic Sensors

- Radio atmospherics (sferics) are RF pulses produced by breakdown activity from 0.1 Hz-10 MHz.
    - Low signal attenuation means these can be detected from 100s of km range - strongest in VLF 3-30 kHz
- Charge is induced on the antenna's flat plate by varying fields
    - Plate is discharged via adjustable RC circuit
    - Current is integrated to obtain a voltage proportional to the applied field
- The circuit's decay time can be adjusted to filter fluctuations τ = RC

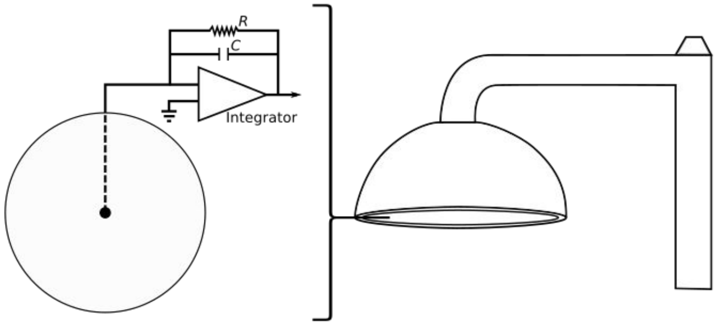

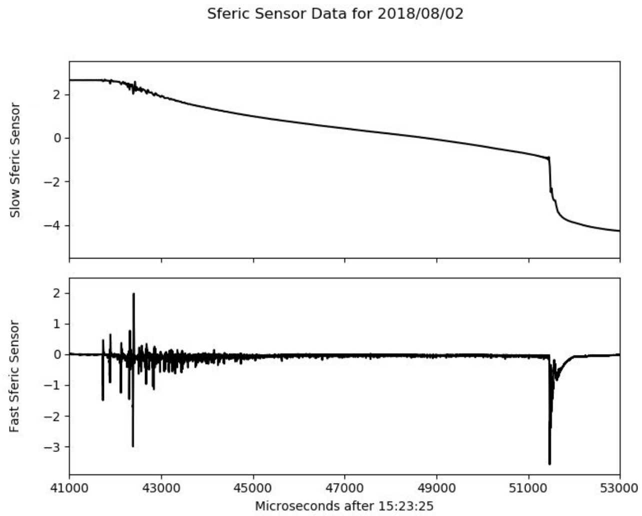

τ = 10 s

τ = 100 μs

Instrumentation:
Broadband Interferometer (INTF)

- Similar to the sferic sensors, the INTF collects induced charge and reads the voltage
- No RC circuit or integrator, sensitive to VHF impulses 20-80 MHz produced by small-scale breakdown
- Identifies 2D source positions (a few per μs)
- Typical errors:
  - ~100 ns in t
  - ~ 0.1° in elv, azi

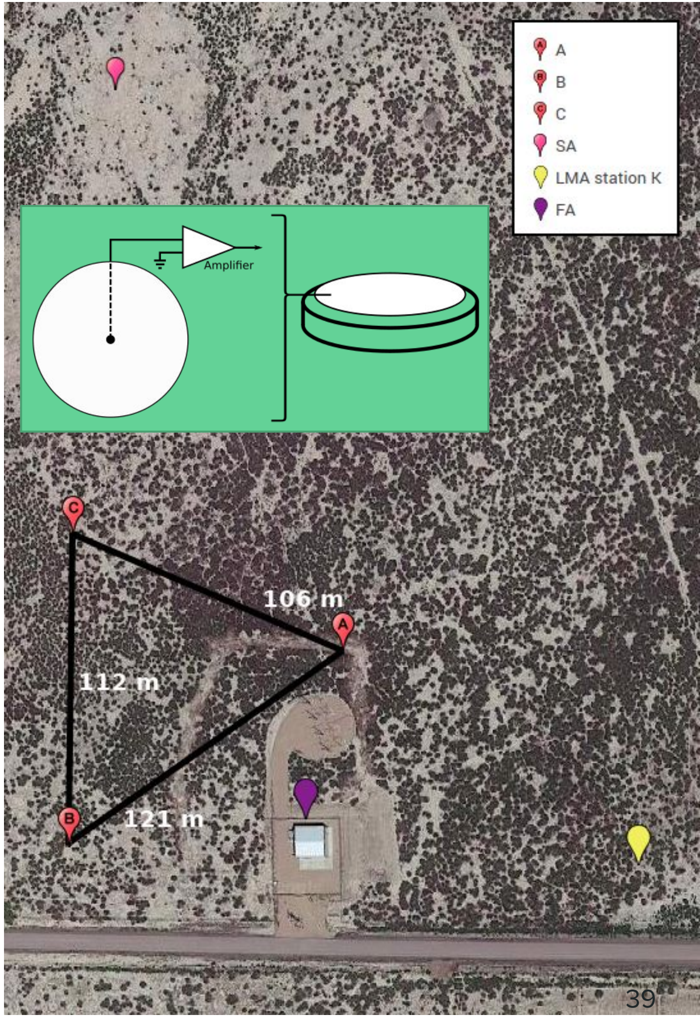

2018 TGFs: Analysis Errors

- Coordinates of TGF sources are determined by four measurements:
  - x, y (LMA) standard error of all LMA points within ±1 ms = $\sigma_{\bar{x}} = \frac{\sigma}{\sqrt{n}}$
  - t (TASD) uncertainty in TASD trigger time = 40 ns
  - z (INTF) standard error of INTF points within ±4 μs = $\sigma_{\bar{x}} = \frac{\sigma}{\sqrt{n}}$
- Standard error can be propagated through iterative method using:

$$\delta f = \sqrt{\left(\frac{\partial f}{\partial x_1}\delta x_1\right)^2 + \ldots + \left(\frac{\partial f}{\partial x_n}\delta x_n\right)^2}$$

- Resulting average errors:
  - Horizontal (x,y): 140 m
  - Vertical (z): 25 m
  - Timing (t): 0.6 μs

Event	D (km)	z_a (km)	t_a (μs)	z_{FNB} (m)	t_{FNB} (μs)	v_{FNB} (m/s)
TGF A	16.96 ± 0.15	3.21 ± 0.03	616,981.7 ± 0.6	150	10.0	1.5×10^7
TGF B	16.64 ± 0.08	2.92 ± 0.02	42,331.7 ± 0.3	100	3.7	2.7×10^7
TGF C	15.98 ± 0.04	2.77 ± 0.01	913,935.1 ± 0.2	120	4.7	2.6×10^7
TGF D	23.9 ± 0.3	3.02 ± 0.04	688,600.1 ± 1.4	240	13.4	1.8×10^7

Effect of each measurement on final solution of TGF A

Measurement	Value	Error	1σ effect on z_a	1σ effect on t_a
x_a (km)	-4.6	0.187	0.010 km (33%)	0.22 μs (37%)
y_a (km)	-16.3	0.143	0.026 km (87%)	0.24 μs (39%)
t_b (μs)	616,987.25	0.04	0 km (0%)	0.04 μs (6.7%)
θ (deg)	10.73	0.026	0.002 km (6.7%)	0.01 μs (1.6%)

2018 TGFs: Results

- Strongest burst of each TGF occurs during the strongest IBP
- Leader step development is faster, stronger, and more linear
  - Power and speed of leader propagation indicates fast negative breakdown (FNB)
- IBPs also have strong sub-pulses, sometimes correlated with TGF production
- Step discontinuity in leader propagation during each TGF onset

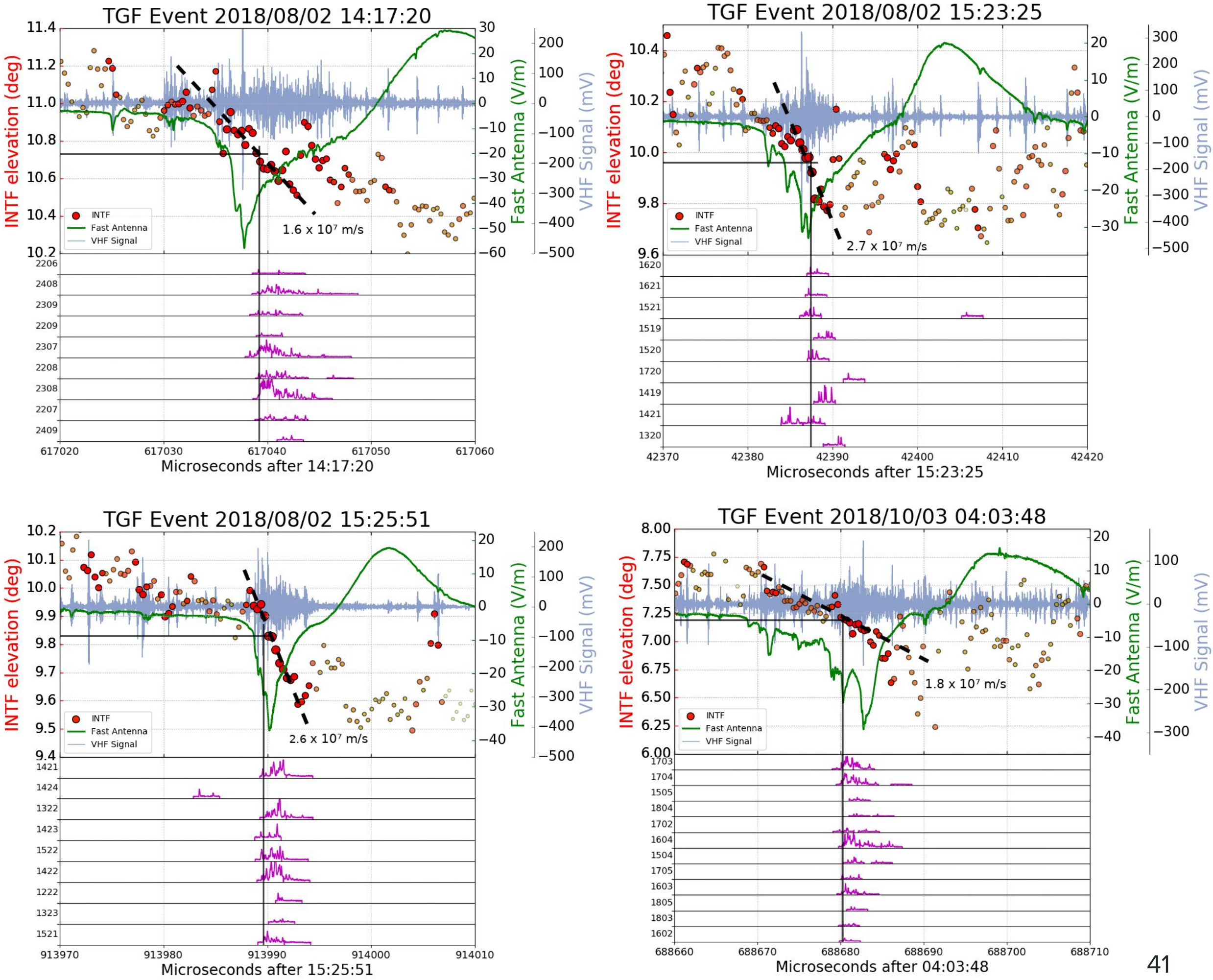

2018 TGFs: Comparison to upward flashes

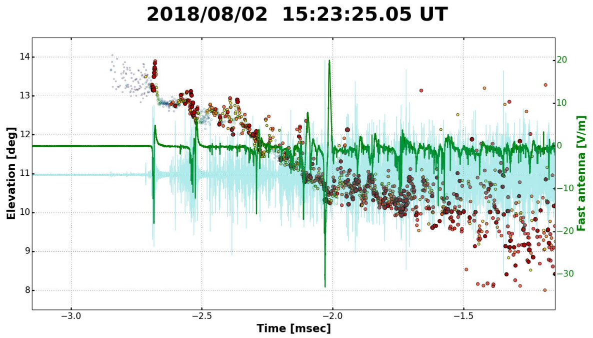

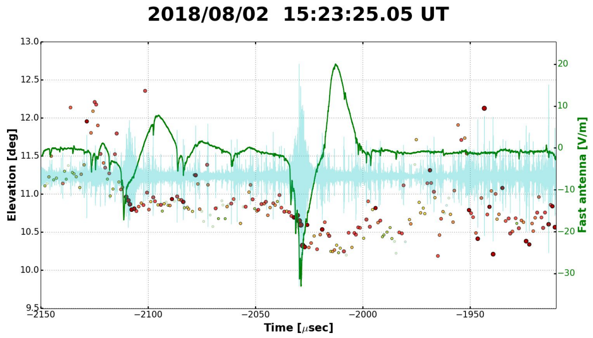

Downward TGF-producing cloud-to-ground flash

- Downward TGFs consist of 10^{12}-10^{14} photons
- Durations of 5-10 μs

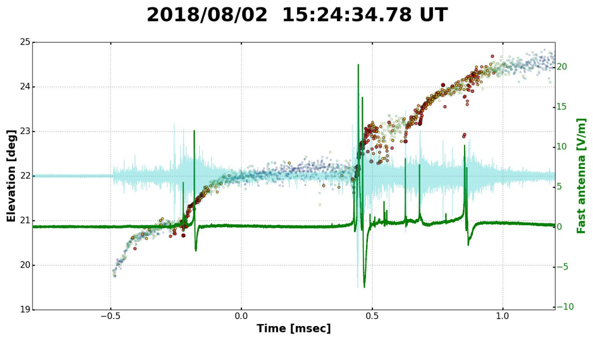

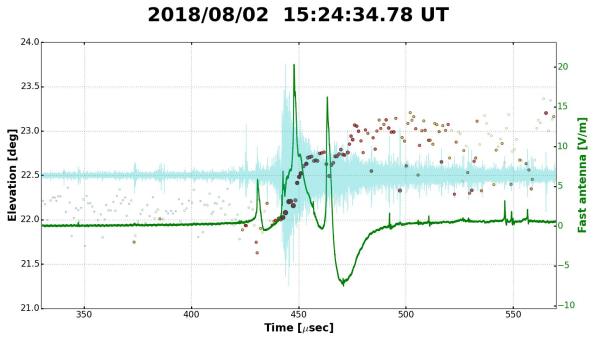

Upward intracloud flash ~1 minute later

- Upward TGFs consist of 10^{15}-10^{19} photons
- Durations of 20-200 μs

2018 TGFs: Comparison to upward flashes

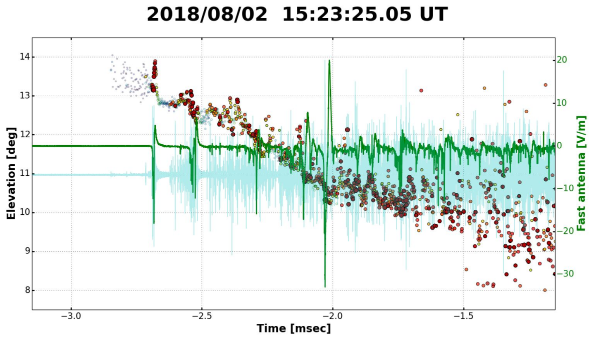

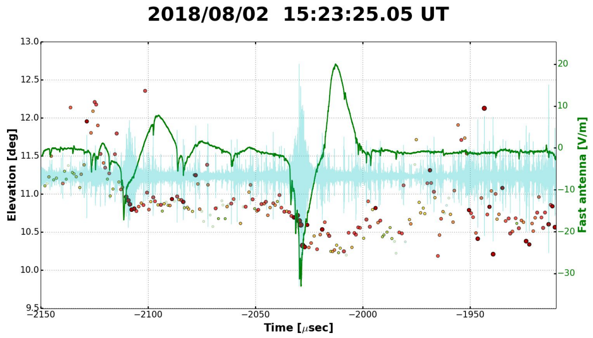

Downward leader steps (0-5 km)

- Step lengths 3-50 m
- Durations of 5-50 μs
- Average speeds 1-30 x 10^5 m/s

(Malan et al. (1935))

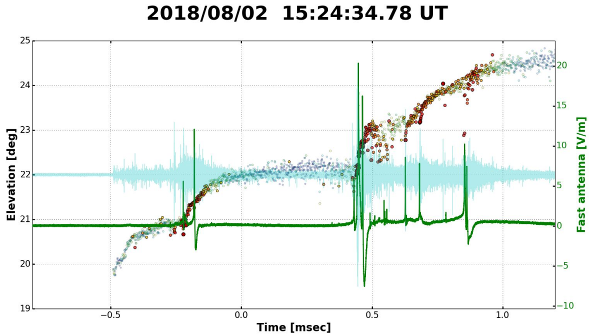

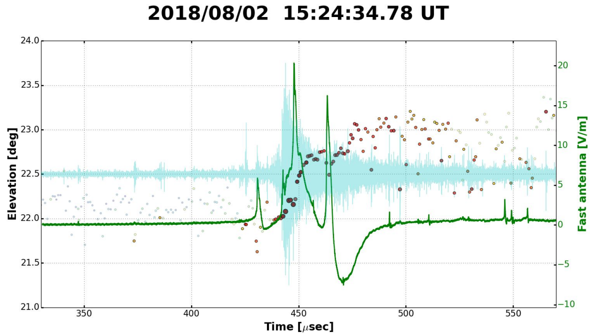

Upward leader steps (10 km)

- Step lengths >200 m
- Durations of ~4 ms
- Average speeds ~10^4 m/s

(Edens et al. (2014))

Optical Camera - Positive Cloud-to-ground Flash

Phantom V2012
40,000 FPS

Aug. 18, 2021
10:25:50 UTC